Biochimica et Biophysica Acta, 1144 (1993) 426–433

BBABIO 43904

Matrix ENDOR of tyrosine D^+ in oriented Photosystem II membranes

Hiroyuki Mino [a], Jun-ichi Satoh [a], Asako Kawamori [a], Kazumi Toriyama [b] and Jean-Luc Zimmermann [c]

[a] *Faculty of Science, Kwansei Gakuin University, Nishinomiya (Japan),* [b] *Government Industrial Research Institute, Nagoya (Japan) and* [c] *Section de Bioénergétique (URA CNRS 1290), Département de Biologie Cellulaire et Moléculaire, Centre d'Etudes de Saclay, Gif sur Yvette (France)*

(Received 27 April 1993)

Key words: Photosynthesis; ENDOR; Photosystem II; Tyrosine D^+; Surrounding proton; Delocalized spin model

Proton matrix ENDOR spectroscopy has been used to probe the proton environment of the stable tyrosine D^+ radical present in Photosystem II membranes. ENDOR spectra in randomly oriented and oriented membranes are reported. Simulations of the spectra are given using both the point dipole approximation and the spin distribution over the tyrosine radical, which were found to provide reasonably good fits. The following results are reported: (1) Five groups of protons can be detected in the matrix ENDOR spectra of D^+, that have ENDOR peak separations less than 2 MHz, and are located at distances between 3.5 and 6.7 Å from the center of the tyrosine ring. These protons are directed approximately parallel to the PS II membrane plane. (2) Three pairs of ENDOR lines with separations of 2.9, 4.1 and 4.7 MHz, are also reported, together with a signal from the hydrogen bonded to the terminal oxygen in the tyrosine molecule. These protons can be exchanged by treatment in a deuterated buffer. From the orientation dependence of these ENDOR lines, it is concluded that they correspond to protons with distance vectors from the ring center that are perpendicular to the PS II membrane plane. We suggest that this specific organization of protons around the tyrosyl D^+ radical contributes to the particular orientation of the β-CH_2 group in the radical, and may also play a role in the unusual stability of the D^+ radical form in the PS II membrane.

Introduction

Oxygen evolution in plant photosynthesis is accomplished by a protein pigment complex called Photosystem II (PS II) [1]. Two tyrosine residues have recently been identified as redox-active components of the PS II electron-transport chain [2–5]. One of them, Y-161 of the D1 polypeptide is called Z, the component which reduces the oxidized reaction center chlorophyll, $P680^+$, and transfers the oxidizing equivalents to the oxygen-evolving complex [2,3]. The other, Y161 in the D2 polypeptide, corresponds to the component D on the donor side of PS II which was first identified as Y160 of the D2 protein in the cyanobacterium *Synechocystis* 6803 [4] and has a stable radical state D^+ with indefinite function [5].

The latter radical gives rise to an EPR signal centered at g approx. 2 known as Signal II_s [6] with a lifetime of the order of hours [7,8]. Results obtained at Q band EPR spectroscopy (35 GHz) have shown that Signal II_s has a slightly anisotropic g tensor with $g_{xx} = 2.0074$, $g_{yy} = 2.0044$ and $g_{zz} = 2.0023$ [9], and displays a hyperfine pattern of four lines arising from coupling with protons. The EPR signal has been simulated using hyperfine coupling constants of approx. 6–7 G with two ring protons, and of approx. 10–11 G with one β-methylene proton from the tyrosine molecule [10]. Using ESEEM spectroscopy, Evelo et al. [11] determined a first proton coupling with $A_{iso} = 27.2$ MHz (approx. 9.7 G) and a small anisotropic component $T_{11} = -3.1$ MHz, which they ascribed to coupling with one of the β-methylene protons, and a second proton coupling with $A_{iso} = \pm 1.6$ MHz and $T_{11} = \mp 8.4$ MHz. This latter proton was shown to be easily exchanged with deuteron [11]. More recently, Barry et al. [12] showed by specific deuteration of the tyrosine D^+ that

Correspondence to: A. Kawamori, Faculty of Science, Kwansei Gakuin University, Uegahara 1-1-155, Nishinomiya 662, Japan.

Abbreviations: PS II, Photosystem II; P680, the primary electron donor of PS II; D, a tyrosine electron donor in D2 subunit of PS II; Z, a tyrosine electron donor in D1 subunit of PS II; Chl, chlorophyll; Tris, 2-amino-2-(hydroxymethyl)1,3-propanediol; Mops, 4-morpholinopropanesulfonic acid; EDTA, ethylenediaminetetraacetic acid; EPR, electron paramagnetic resonance; ENDOR, electron nuclear double resonance; ESEEM, electron spin echo envelope modulation.

the large coupling with $A_{iso} = 10.5$ G ($\cong 29.4$ MHz) that is detected in the EPR spectrum corresponds to coupling with one of the β-methylene protons while the smaller proton coupling with $A_{iso} = 4$ G is due to coupling with protons at positions 3 and 5 of the tyrosine ring. The latter study confirmed the assignment of D^+ as a tyrosyl radical with the high spin density at the *ortho* and *para* positions to the phenol oxygen following an odd-alternant pattern. This odd alternant spin density distribution is also found in tyrosyl radicals produced in vitro [12] and in the tyrosyl free radical present in ribonucleotide reductase from *Escherichia coli* [13]. However, Barry et al. [12] showed that the characteristic lineshape of Signal II_s, from the comparison with that of the tyrosine radical produced by UV irradiation, was arising from the specific conformation of the β-methylene group with respect to the phenol ring, and that this property may be relevant to the specific biological functions of the D^+ radical in PS II.

EPR studies on oriented PS II membranes distinguish two apparent g values, $g_{\|} = 2.0061$ and $g_{\perp} = 2.0031$ [14]. This result, together with the EPR results obtained on a γ-irradiated single crystal of tyrosine-HCl [15], indicates that the orientation of the tyrosine-D phenol ring in the PS II membrane is such that the terminal C-O bond in the tyrosine molecule lies along the membrane normal.

While it is clear from all these studies that the conformation of the tyrosine D component and its close environment in the PS II membranes both play a crucial role in maintaining its unique biological properties, it has also been demonstrated that the unpaired electronic spin density distribution on the D^+ radical are essentially the same as in other tyrosine radicals [12]. Thus, the fine tuning of the biological properties of tyrosine D^+ may be governed by other aspects of its environment. Indeed, the exchangeable protons detected by Rodriguez et al. [16] by ENDOR and by Evelo et al. [11] by ESEEM spectroscopies have been proposed to play a role in the unusual stability of the D^+ radical species [17].

Proton matrix ENDOR spectroscopy provides information on the dipolar interactions between the electronic spin and surrounding protons, such as those from the immediate protein environment. Thus, results on Signal II_s may provide a way to investigate the binding pocket of Y-161 and give clues about the origin of its biological properties. In this respect, Babcock et al. [16,18] reported a matrix ENDOR spectrum of Signal II_s and determined the frequency separation of several pairs of lines. However, no further analysis of the ENDOR spectra was provided. Simulation of matrix ENDOR spectra is generally difficult due to complication by ENDOR enhancement factors that are related to nuclear relaxation mechanisms [19]. It is possible, however, to carry out a simulation by assuming a simplified model based on the angular independent ENDOR responses [20,21]. In this paper, we report detailed matrix ENDOR spectra of D^+ that show a number of lines not found in the published spectra, together with spectra obtained in oriented PS II membranes. The spectra are analyzed using a spin density distribution over the tyrosine D^+ radical similar to that determined by Bender et al. [13] for the tyrosyl radical in ribonucleotide reductase.

Materials and Methods

Oxygen-evolving PS II membranes (400–600 μmol O_2/mg Chl per h) were prepared from market spinach by the method of Kuwabara and Murata [22]. The final pellet was resuspended at about 10 mg Chl/ml in a buffer medium containing 0.4 M sucrose, 20 mM NaCl and 20 mM Mops/NaOH (pH 6.8). EPR samples in calibrated quartz tubes were prepared with the final pellet and were equilibrated in the dark for 15 min before being frozen at 77 K. For the orientation dependence experiments, PS II membranes were suspended in a buffer (0.4 M sucrose, 20 mM NaCl, 5 mM $CaCl_2$, 2 mM EDTA and 20 mM Mops/NaOH at pH 6.8) and dried on pieces of mylar sheets at 4°C for 12–16 h using nitrogen gas and controlled humidity [14]. 6–8 2.5×25 mm^2 pieces of dried mylar sheets were put into an EPR tube, which was subsequently frozen to 77 K. The mylar was tested to give no EPR signal under the conditions used in this study. In order to identify couplings from exchangeable protons, PS II membranes were incubated in the deuterated buffer for 6 days at 8°C after treatment with Tris [16].

The ENDOR spectra were recorded on a Varian E-109 EPR spectrometer equipped with a home made ENDOR system. ENDOR signals were measured using modulation of the NMR frequency at 10 kHz. The rf power of 250 W from an ENI 3200L power amplifier was supplied to 12 lines of ENDOR coils parallel to the cylindrical axis of a TE_{011} cavity, and terminated with a 50 Ω dummy load. The rf voltage across the dummy load was monitored on an oscilloscope to check the rf magnetic field produced by the current through the coils. Experiments were performed at 100 K using a home made cryostat operating with cold nitrogen gas, or at 10 K using an Oxford Instruments liquid helium cryostat.

Results and Discussion

Fig. 1 shows the ENDOR spectrum of Signal II_s observed in a randomly oriented (powder-like) sample of PS II at 100 K. This ENDOR spectrum was obtained at the zero cross-field position (3356 G) in the field modulated EPR signal (see Fig. 1, inset). Five

pairs of ENDOR lines are clearly identified in the spectrum that are labelled as AA′, BB′, CC′, EE′ and FF′. The lines in each doublet are separated by 0.19, 0.47, 0.75, 1.23 and 1.75 MHz, respectively. The center position of each doublet is close to the free proton frequency $\nu_p = 14.3$ MHz. Consequently these ENDOR lines are assigned to dipolar couplings of the D^+ electronic spin with the surrounding matrix protons. Proton matrix ENDOR spectra of Signal II_s were obtained in the oriented PS II membranes with different orientations of the external magnetic field vector with respect to the membrane normal (ζ angle). The spectra are displayed in Fig. 2 which shows that the positions of the ENDOR lines are only slightly affected by changes in direction of the magnetic field, while the intensities of each pair of lines vary with the direction of the magnetic field. Similar changes in the intensity of ENDOR lines has been observed by Mustafi et al. [23] in a randomly oriented sample of a spin-labelled amino acid. This intensity variation corresponds to different orientations of a radical with respect to the magnetic field in a randomly-oriented sample but can be observed more clearly by variation of the magnetic field direction in an oriented sample.

The pairs AA′, CC′ and DD′ have maximum intensity with the membrane normal parallel to the magnetic field direction, and minimum intensity with the membrane normal perpendicular to the magnetic field.

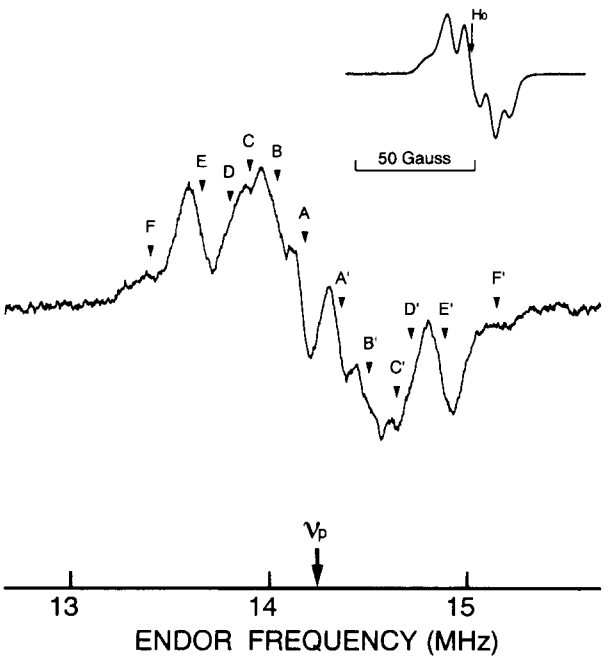

Fig. 1. Matrix ENDOR spectrum of Signal II_s obtained in a randomly oriented sample. The magnetic field was fixed at $H_0 = 3356$ G. The inset shows the EPR signal with the arrow indicating the fixed H_0 used for the ENDOR observation. ENDOR conditions: temperature, 100 K; microwave power, 0.5 mW; modulation frequency, 10 kHz; frequency modulation depth, 30 kHz; rf power, 250 W.

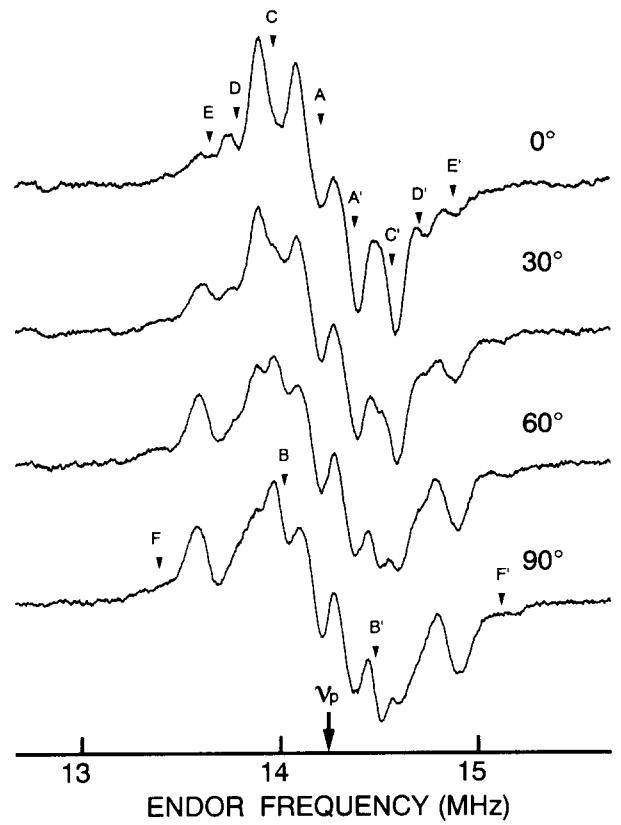

Fig. 2. Matrix ENDOR spectra of Signal II_s obtained in oriented PS II membranes at different orientations of the external magnetic field vector with respect to the membrane normal (angle ζ). The other experimental conditions are the same as in Fig. 1.

The intensities of the other three line pairs BB′, EE′ and FF′ vary with opposite tendency. These results are summarized in Table I.

TABLE I

ENDOR peak separations in oriented and randomly-oriented PS II membranes (MHz)

The values shown in parentheses give relative intensities in each direction which were estimated by experimental derivative peaks and normalized by the total area of integrated ENDOR intensity within 3 MHz, with its center at the free proton frequency. Each distance was estimated by Eq. 1 for ENDOR separations corresponding $\theta = 90°$ ($A_\perp$ components) in the randomly-oriented sample.

Peak	AA′	BB′	CC′	DD′	EE′	FF′
0°	0.23		0.62	0.95	1.23	
	(6.4)		(9.4)	(4.0)	(2.5)	
30°	0.17	0.50	0.65	0.95	1.20	1.63
	(2.7)	(6.6)	(9.4)	(3.8)	(3.6)	(1.0)
60°	0.16	0.47	0.67	0.94	1.20	1.70
	(2.3)	(7.5)	(8.4)	(3.8)	(3.5)	(1.2)
90°	0.14	0.46	0.70		1.20	1.80
	(1.4)	(6.7)	(8.3)		(3.2)	(1.2)
Randomly-oriented sample	0.19	0.47	0.75		1.23	1.75
	(0.8)	(4.0)	(4.9)		(3.2)	(1.2)
Distance (Å)	7.5	5.5	4.7		4.0	3.6

Approximate distances between the protons contributing to the ENDOR lines and the D^+ radical can be estimated, if in a first approximation it is assumed that the electronic spin is localized at the center of the tyrosine ring. Since we are dealing with protons weakly coupled to the electronic spin, it can also be approximated that the isotropic part of the hyperfine coupling constants is negligible. In this case the ENDOR peak separation can be related to the dipolar interaction between a proton and the electronic spin by

$$\Delta\nu = g_n\beta_n g\beta(1-3\cos^2\theta)/R^3 \quad (1)$$

where θ is the angle between the external magnetic field vector $\mathbf{H_0}$ and the electron-nucleus distance vector **R**. In a powder pattern intense contributions are usually observed from the 90° orientation ($A_\perp$ component) [24]. This property is illustrated here by the fact that the ENDOR spectrum of the oriented sample with $\zeta = 90°$ (Fig. 2, bottom trace) is very similar to that of the randomly oriented sample (Fig. 1). From the results of the ENDOR spectrum obtained for the randomly oriented PS II membranes and making $\theta = 90°$ in Eqn. 1, the following distances can be calculated for five groups of protons: 7.5 Å for AA′, 5.5 Å for BB′, 4.7 Å for CC′, 4.0 Å for EE′ and 3.6 Å for the FF′ pair, respectively. These results are summarized in Table I.

Kevan et al. [20,21] have shown that the angular dependence of the transition probability can be neglected when simulating the matrix ENDOR from protons at distances between 3 and 5 Å from the electronic spin. When this assumption is made, the signal amplitude is proportional to an enhancement factor $F(R,N_R)$ that depends on both the distance R and the number of protons N_R at that distance. The simulated ENDOR spectrum of oriented PS II membranes can be obtained by assuming a Gaussian distribution of membrane orientations according to

$$R(\zeta) = (2\pi\Delta^2)^{-1/2}\exp(-(\zeta_0-\zeta)^2/2\Delta^2) \quad (2)$$

where ζ_0 is the mean angle between the membrane normal and the magnetic field and Δ is the mean square deviation from the mean which we take here as 15° [25]. Taking the Gaussian line broadening into

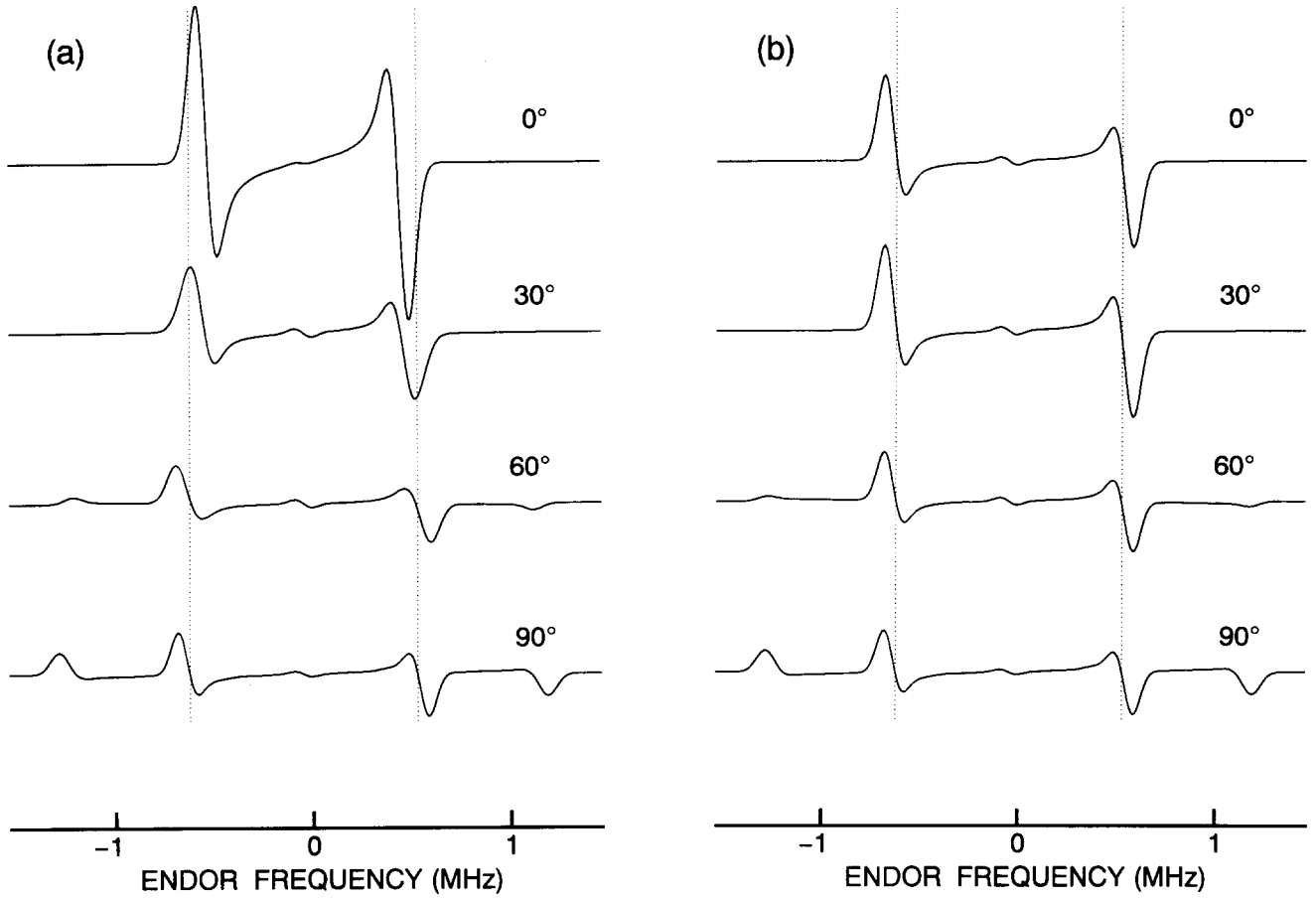

Fig. 3. Theoretical ENDOR spectra for a single proton located at a distance $R = 4$ Å from the ring center with the angle between the **R** vector and the membrane normal $\Theta = 90°$. The external magnetic field is varied from $\zeta = 0°$ to $\zeta = 90°$. The spectra were calculated using the delocalized model (a) and the localized model (b) described in the text (see Scheme I).

consideration for each component line, the ENDOR line shape can be computed with the following formula

$$S(\nu-\nu_0)=\Sigma_k \frac{\iiint F(R,N_R)R(\zeta)g(\nu')\sin\zeta\,d\zeta\,d\phi\,d\nu'}{\iint R(\zeta)\sin\zeta\,d\zeta\,d\phi} \quad (3)$$

in which the summation k is carried out over all the possible distances of protons under resonance, and $g(\nu')$ is the Gaussian line broadening

$$g(\nu')=(2\pi b^2)^{-1/2}\exp(-(\nu-\nu')^2/2b^2) \quad (4)$$

b is estimated to be 45 kHz based on the linewidth of the observed ENDOR lines.

In the system studied here, the electron spin is not localized at the center of the tyrosine ring but rather delocalized over the whole tyrosine molecule. If we consider the distribution of electron spin density over the six carbons and one oxygen of the molecule, then Eqn. 1 must be replaced by the following for the frequency separation related to the i-th proton

$$\Delta\nu_i=g_n\beta_n g\beta\Sigma_j(1-3\cos^2\theta_{ij})\rho(j)/R^3{}_{ij} \quad (5)$$

where $\rho(j)$ is the electronic spin density on the j-th carbon atom in the molecule. R_{ij} is the distance between the i-th proton and the j-th carbon and θ_{ij} is the angle between the distance vector $\mathbf{R_{ij}}$ and $\mathbf{H_0}$.

We have performed simulations of the ENDOR spectra using the spin density distribution on the tyrosine molecule derived from the ENDOR study of the tyrosyl radical in ribonucleotide reductase [13]. The positions of the carbon and oxygen atoms were taken from Ref. [26]. As mentioned above, it was found that for Signal II_s, the apparent g value of 2.0061 corresponds to the orientation parallel to the normal of the PS II membranes [9], and in the EPR spectrum of γ-irradiated tyrosine-HCl crystals the $g=2.0067$ direction lies along the C-O bond [15]. This indicates that the C-O bond lies along the membrane normal.

Fig. 3a and 3b show the simulated ENDOR spectra obtained for a proton located at a distance $R=4$ Å from the ring center with the vector connecting the ring center and the proton making an angle $\Theta=90°$ with the membrane normal (see Scheme I), when the angle ζ between the membrane normal and the external magnetic field is varied from 0° to 90°. For the simulation shown in Fig. 3a and 3b, the distance vector **R** connecting the center of the tyrosine ring and the proton was taken perpendicular to the plane of the ring, but similar results were obtained for other directions (not shown). The results of the simulations done for the delocalized model indicate that the positions of the two lines corresponding to the coupling constant $A_\perp$ for a proton with $\Theta=90°$ move towards outside

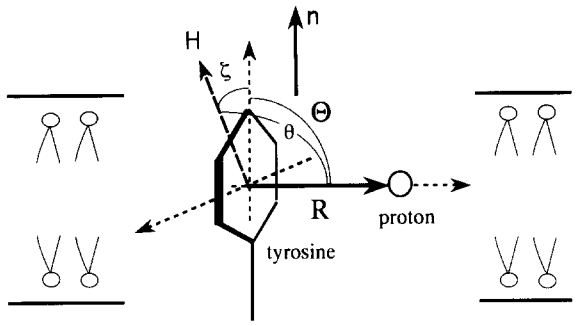

Scheme 1.

the center of the spectrum with increasing ζ (Fig. 3a). However, in the localized model these peaks do not change frequency when ζ is changed (Fig. 3b). On the other hand, when the **R** vector is directed parallel to the membrane normal ($\Theta=0°$), both models predict that the amplitudes of the corresponding ENDOR lines vary when the direction of the external magnetic field is changed. This indicates that the $A_\parallel$ and $A_\perp$ components are observed with maximum amplitudes with $\zeta=0°$ and $\zeta=90°$, respectively.

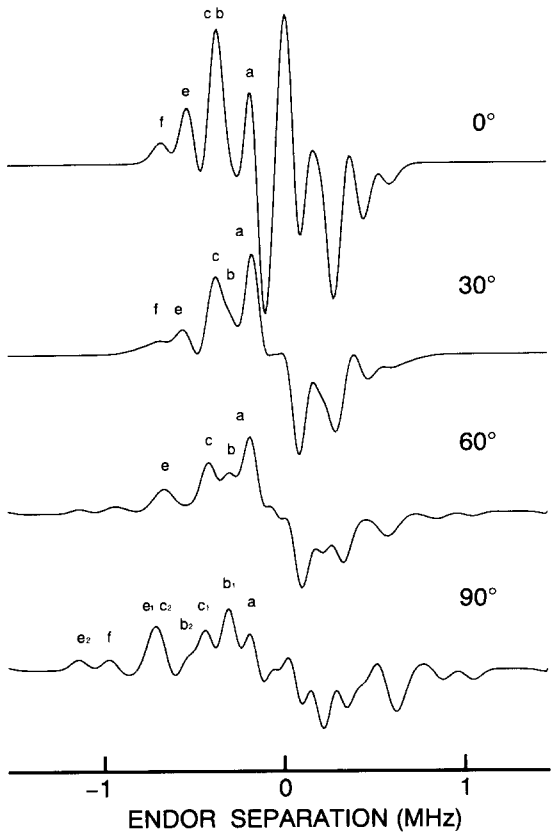

Fig. 4. Angular dependence of the simulated ENDOR spectra based on the distances, angles and enhancement factors shown in Table II, the spin density distribution given in Ref. 13 and the lattice parameters in Ref. 26. The spectra reproduce most of the features shown in the experimental spectra (Fig. 2).

TABLE II

Parameters of position of protons R, Θ and ENDOR enhancement factors $F(R,N_R)$

Peak signs correspond to those in randomly-oriented PS II membranes.

Peak sign	aa′	bb′	cc′	ee′	ff′
Distance (Å)	6.7	5.2	4.8	4.0	3.5
Θ (deg)	90	83	90	86	83
Enhancement factor	1.0	0.8	1.2	0.8	0.5

Based on these results we performed simulations of the ENDOR spectra obtained for the D^+ radical. The simulations best reproducing the experimental spectra are shown in Fig. 4 which was obtained using the geometrical parameters listed in Table II. These results indicate that the ENDOR spectra can be reasonably simulated using five protons at distances between 3.5 Å and 6.7 Å from the tyrosine ring center. These distances obtained by the simulations of the ENDOR spectra of the D^+ radical in oriented membranes are quite close to the distances that could be estimated with a simple dipole model (see Table I). The small differences that can be observed for the assignments of the line pairs AA′ and BB′ may be due to the angular dependence of the enhancement factor that may not become negligible at these distances and this was not taken into account in our simulations.

The simulation also indicates that all the matrix ENDOR protons detected here lie at positions with Θ approx. 90° (Table II), i.e., with **R** vectors perpendicular to the direction of the C-O bond. Note that the use of the delocalized model to simulate the ENDOR spectra results in distances shorter by only up to 20% compared to those obtained with the localized model, depending on the positions of the protons. In fact, it is shown in Fig. 2 that the positions of the matrix ENDOR lines are only slightly affected by the direction of the magnetic field in membrane-oriented spectra. This indicates that the more simple localized model is adequate to estimate approximate distances of protons from the tyrosine radical. To deduce the correct features of the matrix ENDOR spectra of D^+, such as shown in Fig. 3a, the spin delocalized model should be taken into account.

Fig. 5A shows the matrix ENDOR spectrum of D^+ recorded at 10 K over a broader frequency range. Additional features can be detected in this spectrum that were not observed at 100 K (Fig. 1). A number of these new peaks can be paired as GG′, HH′ and II′. The corresponding ENDOR peak separations are shown in Table III. These new peaks correspond to couplings with protons located at closer distances (larger coupling constants) than those observed in the

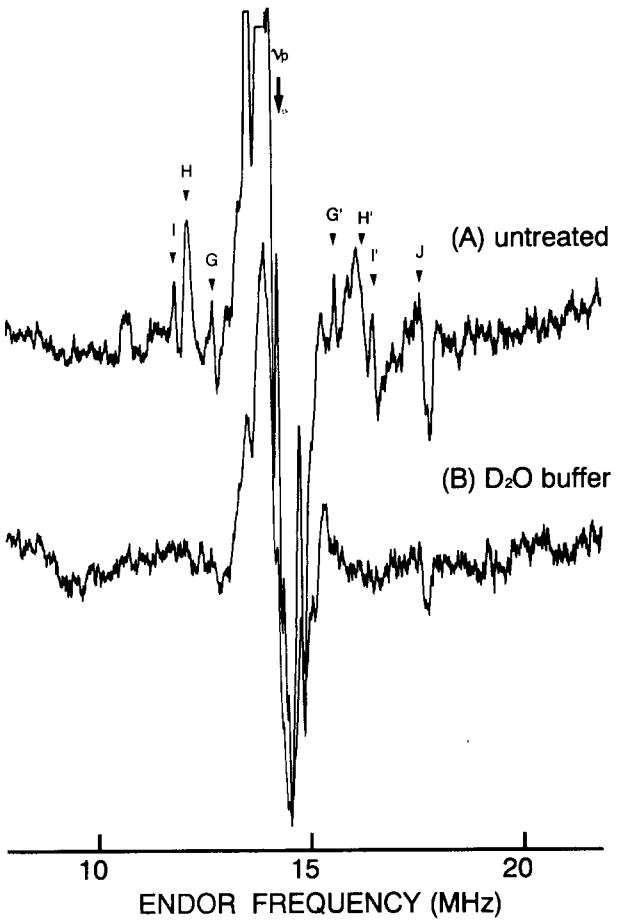

Fig. 5. Matrix ENDOR spectra of Signal II_s obtained over a 10 MHz frequency range. Spectrum (A) was obtained in the untreated sample and spectrum (B) in the sample treated with the deuterated buffer. The experimental conditions were the same as in Fig. 1, except for the microwave power (1 mW) and the temperature (10 K).

spectrum recorded at 100 K (see Fig. 1). In addition, these three ENDOR line pairs are not observed in the sample that has been incubated with D_2O (Fig. 5B). This result rules out the possibility that these new peaks correspond to protons from the tyrosine molecule, because these would not be expected to be exchanged by the deuteration procedure. Some of these results have been observed and reported earlier [16,18]. Another peak labelled J in Fig. 5 is present in the

TABLE III

ENDOR peak separations in oriented and randomly-oriented PS II membranes (MHz)

Peak sign	GG′	HH′	II′	J	K
0°	2.95	4.03	4.69	–	8.81
30°	2.93	3.99	4.74	6.59	8.82
60°	2.91	4.00	4.70	6.99	–
90°	–	3.80	–	7.01	–
Non-oriented	2.90	4.07	4.70	6.99	–
Babcock et al. [18]	(2.5) 3.2	3.5 3.9	5.0 (5.9)	7.1	9.4

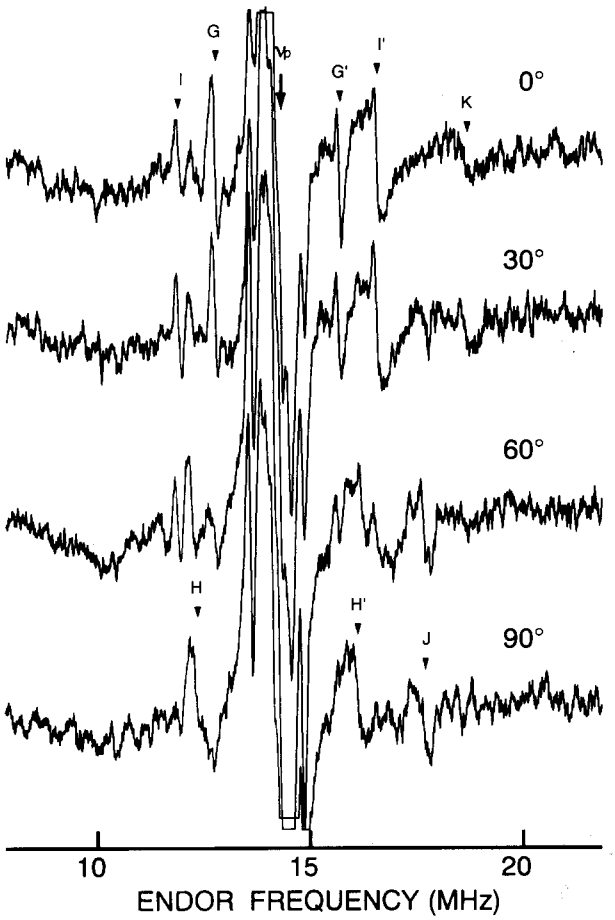

Fig. 6. Matrix ENDOR spectra of Signal II_s obtained in an oriented sample. The experimental conditions were the same as in Fig. 5.

ENDOR spectrum of which intensity is smaller after the treatment with D_2O, though it disappeared by treatment at a higher pH buffer [16]. This peak corresponds to a hyperfine coupling constant of approx. 7.0 MHz, and can be assigned to coupling with a hydrogen bonded to the terminal oxygen in the tyrosine molecule, based on a similar coupling detected by ESEEM spectroscopy [11]. Pertinent to this hydrogen, the angular dependence of the ENDOR lines shown in Fig. 6 indicates that its direction from the ring center is approximately along the membrane normal, because the component A_{11} appears at $\zeta = 90°$. Whether or not the O-H bond lies in the same plane as the tyrosine ring, the distance vector of the O-H proton from the center of ring makes the angle Δ of approx. 20° with the membrane normal, if we take into account that the C-O bond lies parallel to the membranes normal and the angle COH is 110° [26].

The ENDOR lines labelled GG′, HH′ and II′ in Fig. 5A correspond to couplings with protons that are located at closer distances than those given in the simulation shown in Fig. 4. In the present case, however, a meaningful simulation and the determination of correct distances are more difficult to perform, since the effect of isotropic hyperfine coupling may not be neglected. However, the angular dependence of the peaks (Fig. 6) can give the following information: (i) the pair II′ corresponds to the coupling $A_{\parallel} = 4.7$ MHz with a proton that is directed approximately parallel to the membrane normal ($\Theta = 0$–30°); (ii) similarly the pair GG′ corresponds to a coupling with $A_{\parallel} = 2.9$ MHz; and (iii) the line labelled K is absent in the spectrum at $\zeta = 90°$, just like the pairs GG′ and II′, whereas the HH′ pair is more intense at $\zeta = 90°$. Since K and HH′ vary with opposite tendency in the orientation experiment, it is possible that they correspond to couplings to the same proton with $A_{\perp} = 3.8$ MHz and $A_{\parallel} = 8.8$ MHz. If this is the case, then the hyperfine coupling constants with this proton are $T_{\perp} = \mp 4.2$ MHz, $T_{\parallel} = \pm 8.4$ MHz and $A_{iso} = \pm 0.4$ MHz, with the proton directed toward the membrane normal, i.e., in the direction of the C-O bond.

The analysis of proton matrix ENDOR spectra presented in this paper shows that the point dipole approximation given in Eqn. 1 in randomly oriented membranes is quite adequate to derive approximate distances of matrix protons located at 3.5 to 6.7 Å from the tyrosyl D^+ radical center. The angular dependence of the intensity of each ENDOR line in samples from oriented membranes gives information about not only the distances but also the directions of protons from the radical center. Calculations using the spin density distribution over the tyrosyl radical yield distances that are different by only up to 20% for the protons in the matrix region.

The analysis presented here is based on the spin density distribution on the tyrosyl radical in ribonucleotide reductase from *E. coli* which is close to that expected for the tyrosyl D^+ radical in PS II studied here [12]. As mentioned above, however, a remarkable difference between the two radicals is found in the orientation of the β methylene group with respect to the tyrosine ring plane. The particular orientation found for the PS II tyrosine D^+ radical suggests a steric hindrance from surrounding atoms. In this respect, it is worth noticing that all the protons detected in the matrix region by the present study and lying at distances 3.5 Å to 6.7 Å from the ring center (AA′ to FF′ in Table II) are located in the direction normal to the ring plane. We suggest that the presence of these protons may contribute to the particular orientation of the β CH_2 group in D^+.

In addition, the ENDOR results obtained over a broader frequency range and at lower temperature indicate that protons located at closer distances are also coupled with the electronic spin. For these protons, contact hyperfine coupling interactions may not be negligible. This indicates that a more elaborate simulation than that based on Eqn. 1 should be per-

formed to extract meaningful distance information. This work is in progress in our laboratories. Results obtained in oriented PS II membranes indicate that these close protons lie approximately along the membrane normal, which is approximately the direction of the tyrosine C-O bond, contrary to the other set of protons participating in the steric hindrance responsible for the particular orientation of the β CH_2 group in the D^+ radical.

We have recently found that the shape of Z^+ signal is a little different from that of D^+ when measured by field-swept ESE spectroscopy, and the difference have been ascribed to differences in the hyperfine couplings for one of the β-CH_2 proton of the radical [27]. ENDOR spectroscopy has been currently applied in our laboratories to measure the proton environment of Z^+ and to compare it to that determined for D^+. We have found the environment of Z^+ is more flexible than that of D^+ [28]. Svensson et al. [29] have elaborated a molecular model of PS II based on analyses of the protein sequences and computer simulations and suggested that the enveronment of D^+ is more hydrophobic than that of Z^+. We suggest that the matrix protons surrounding the tyrosine D^+ in the direction parallel to the membrane plane may contribute to this character, resulting in the unusual stability of the tyrosyl radical.

Acknowledgement

This work was supported in part by the Monbusho International Scientific Research Program-Joint Research (63044148) from the Ministry of Education, Science and Culture, Japan.

References

1 Rutherford, A.W., Zimmermann, J.-L. and Boussac, A. (1992) in The Photosystems: Structure,Function and Molecular Biology (Barber, J., ed.), pp. 179–229, Elsevier, Amsterdam.
2 Debus, R.J., Barry, B.A., Sithole, I., Babcock, G.T. and McIntosh, L. (1988) Biochemistry 27, 9071–9074.
3 Metz, J.G., Nixon, P.J., Rögner, M., Brudvig, G.W. and Diner, B.A. (1989) Biochemistry 28, 6960–6969.
4 Debus, R.J., Barry, B.A., Babcock, G.T. and McIntosh, L. (1988) Proc. Natl. Acad. Sci. USA 85, 427–430.
5 Vermaas, W.F.J., Rutherford, A.W. and Hansson, Ö. Proc. Natl. Acad. Sci. USA 85, 8477–8481.
6 Babcock, G.T. and Sauer, K. (1973) Biochim. Biophys. Acta 325, 483–503.
7 Styring, S. and Rutherford, A.W. (1987) Biochemistry 26, 2401–2405.
8 Inui, T., Kawamori, A., Kuroda, G., Ono, T.-A. and Inoue, Y. (1989) Biochim. Biophys. Acta 973, 147–152.
9 Brok, M., Ebskamp, F.C.R. and Hoff, A.J. (1985) Biochim. Biophys. Acta 809, 421–428.
10 Barry, B.A. and Babcock, G.T. (1988) Chem. Scripta 28A, 117–122.
11 Evelo, R.G., Hoff, A.J., Dikanov, S.A. and Tyryshkin, A.M. (1989) Chem. Phys. Lett. 161, 479–484.
12 Barry, B.A., El-Deeb, M.K., Sandusky, P.O. and Babcock, G.T. (1990) J. Biol. Chem. 265, 20139–20143.
13 Bender, C.J., Sahlin, M., Babcock, G.T., Barry, B.A., Chandrashekar, T.K., Salowe, S.P., Stubbe, J., Lindstm, B., Petersson, L., Ehrenberg, A. and Sjoberg, B.-M. (1989) J. Am. Chem. Soc. 111, 8076–8083.
14 Rutherford, A.W. (1985) Biochim. Biophys. Acta 807, 189–201.
15 Fasanella, E.L. and Gordy, W. (1969) Proc. Natl. Acad. Sci. USA 62, 299–304.
16 Rodriguez, I.D., Chandrashekar, T.K. and Babcock, G.T. (1987) in Progress in Photosynthesis Reserch, Vol. I (Biggins, J., ed.), pp. 471–474, Martinus Nijhoff, The Hague.
17 Babcock, G.T., Barry, B.A., Debus, R.J., Hoganson, C.W., Atamian, M., McIntosh, L., Sithole, I. and Yocum, C.F. (1989) Biochemistry 28, 9557–9565.
18 Babcock, G.T., Chandrashekar, T.K., Ghanotakis, D.F., Hoganson, C.W., O'Malley, P.J., Rodriguez, I.D. and Yocum, C.F. (1987) in Progress in Photosynthesis Research, Vol. I (Biggins, J., ed.), pp. 463–469, Martinus Nijhoff, The Hague.
19 Brustolon, M. (1989) Advanced EPR (Hoff, A.J., ed.), pp. 593–614, Elsevier, Amsterdam.
20 Kevan, L., Narayana, P.A., Toriyama, K. and Iwasaki, M. (1979) J. Chem. Phys. 70, 5006–5014.
21 Kevan, L., Schlick, S., Toriyama, K. and Iwasaki, M. (1980) J. Phys. Chem. 84, 1950–1954.
22 Kuwabara, T. and Murata, N. (1982) Plant Cell Physiol. 23, 533–539.
23 Mustafi, D., Sachleben, J., Well, G. and Makinen, W. (1990) J. Am. Chem. Soc. 112, 2558–2566.
24 Pake, G.E. (1948) J. Chem. Phys. 16, 327–336.
25 George, G.N., Prince, R.C. and Cramer, S.P. (1989) Science 243, 789–791
26 Frey, M.N., Koetzle, T.F., Lehmann, M.S and Hamilton, W.C. (1973) J. Chem. Phys. 58, 2547–2556
27 Kodera, Y., Takura, K., Mino, H. and Kawamori, A. (1992) in Research in Photosynthesis, Vol. II (Murata, N., ed), pp. 57–60, Kluwer, Dordrecht.
28 Mino, H., Kodera, Y. and Kawamori, A. (1992) in Research in Photosynthesis, Vol. II (Murata, N., ed), pp. 61–64, Kluwer, Dordrecht.
29 Svensson, B., Vass, I. and Styring, S. (1991) Z. Naturforsch. 46c, 765–776.